Hunger-promoting hypothalamic neurons modulate effector and regulatory T-cell responses

Giuseppe Matarese[a,b,1], Claudio Procaccini[a,b], Ciro Menale[c,d], Jae Geun Kim[d], Jung Dae Kim[d,e], Sabrina Diano[d,e,f,g], Nadia Diano[c], Veronica De Rosa[a,b,h], Marcelo O. Dietrich[d,i], and Tamas L. Horvath[d,e,f,g,1]

[a]Dipartimento di Medicina e Chirurgia, Università degli Studi di Salerno, 84081 Salerno, Italy; [b]Laboratorio di Immunologia, Istituto di Endocrinologia e Oncologia Sperimentale and [c]Institute of Genetics and Biophysics, Consiglio Nazionale delle Ricerche, 80131 Naples, Italy; [d]Program in Integrative Cell Signaling and Neurobiology of Metabolism, [e]Section of Comparative Medicine, [f]Department of Obstetrics and Gynecology and Reproductive Sciences, and [g]Department of Neurobiology, Yale University School of Medicine, New Haven, CT 06520; [h]Unità di Neuroimmunologia, Fondazione Santa Lucia, 00143 Rome, Italy; and [i]Department of Biochemistry, Universidade Federal do Rio Grande do Sul, RS 90035, Porto Alegre, Brazil

Edited* by Roger D. Cone, Vanderbilt University School of Medicine, Nashville, TN, and approved March 4, 2013 (received for review June 22, 2012)

Whole-body energy metabolism is regulated by the hypothalamus and has an impact on diverse tissue functions. Here we show that selective knockdown of Sirtuin 1 Sirt1 in hypothalamic Agouti-related peptide-expressing neurons, which renders these cells less responsive to cues of low energy availability, significantly promotes CD4$^+$ T-cell activation by increasing production of T helper 1 and 17 proinflammatory cytokines via mediation of the sympathetic nervous system. These phenomena were associated with an impaired thymic generation of forkhead box P3 (FoxP3$^+$) naturally occurring regulatory T cells and their reduced suppressive capacity in the periphery, which resulted in increased delayed-type hypersensitivity responses and autoimmune disease susceptibility in mice. These observations unmask a previously unsuspected role of hypothalamic feeding circuits in the regulation of adaptive immune response.

immune system | sirtuins

Hypothalamic Agouti-related peptide-expressing (AgRP) neurons are mandatory for feeding and survival (1, 2) and they mediate effects of the hystone deacetylase Sirtuin 1 (Sirt1) on energy metabolism (3, 4). Behavioral and metabolic adaptations to low energy availability are enabled by AgRP neurons, but it is unknown whether these neurons are involved in the regulation of other tissue functions key to survival, such as adaptive immune responses. Sirtuins are NAD$^+$-dependent class-III deacetylases that are highly conserved across species (5). Nutrient deprivation up-regulates Sirt1 in several tissues (6, 7), which is important for the metabolic shift that occurs during negative energy balance (8), a metabolic state in which energy expenditure is higher than energy intake. Evidence suggests that the effects of sirtuins may mediate the beneficial effects of calorie restriction, the only known physiological intervention that promotes a longer, healthier lifespan across species (9–14). However, the site of action of sirtuins in these physiological processes remains ill-defined.

The CNS was previously recognized as an immune-privileged site with lack of immunosurveillance. However, accumulating evidence has shown that a mutual interaction between the immune system and CNS exists both in physiological and pathological situations (15). The CNS influences and controls the immune system at least partly through the autonomic nervous system (15). Lymphocytes express the receptors for different neurotransmitters, which enable the brain to properly coordinate the immune system and to maintain the homeostasis of the whole body by responding to environmental changes, such as infections, in an appropriate manner. In this context, we and others have shown that nutritional status can affect T helper 1 (Th1) proinflammatory immune responses through a series of adipose-tissue-derived hormones including leptin, which mediates its effects on immune cells either directly by activating leptin receptors on T cells or indirectly by its effect on autonomic nervous system.

Recent studies have shown that Sirt1 negatively regulates T-cell activation and plays a major role in clonal T-cell anergy in mice. Up-regulation of Sirt1 expression led to T-cell anergy by diminishing the activity of the transcription factor activator protein 1, through the deacetylation of c-Jun (16).

Conversely, Sirt1-deficient mice were unable to maintain T-cell tolerance and developed severe experimental autoimmune encephalomyelitis (EAE) as well as spontaneous autoimmunity, and treating them with resveratrol (a strong activator of Sirt1) led to decreased disease symptoms as well as inflammatory cell infiltration in the CNS (16). As mentioned above, selective knockdown of Sirt1 in hypothalamic AgRP neurons alters the central perception of hunger, inducing a series of metabolic/behavioral adaptations that resemble those of a satiety phenotype despite reduced food intake and body fat mass (4). Thus, in this study we aimed to determine whether selective ablation of Sirt1 expression in AgRP neurons affects peripheral adaptive immunity by analyzing lymphoid organs' immune phenotype, thymic selection, in vitro/in vivo regulatory/proinflammatory immune responses, and autoimmune disease susceptibility in mice.

Results

Altered Generation of Thymus-Derived, Naturally Occurring Regulatory T Cells in AgRP-Sirt1 Knockout Mice. First we compared the basal immunophenotype of the thymus, bone marrow, lymph nodes, and spleen obtained from AgRP-Sirt1 KO mice and their littermate controls. Sirt1 was equally expressed in highly purified T-cell subsets (effector and regulatory T cells) in experimental and control mice, and its knockout was selective for AgRP neurons (Fig. S1). No significant differences were observed either in basal immune phenotypes or activation markers of the bone marrow, lymph nodes, and spleen of naïve unimmmunized AgRP-Sirt1 KO mice (Figs. S2–S8). However, significant differences were detected in the thymus (Fig. 1). AgRP Sirt1 knockout (KO) mice displayed a more "immature" thymic phenotype: Quantification of CD4- and CD8-positive cells revealed a significant increase in the percentage of double-negative (DN) thymocytes in AgRP Sirt1 KO mice, although the total number of thymocytes was not reduced (Fig. 1 *A*–*C*). We also observed a significant reduction in the percentage of double-positive (DP) CD4$^+$CD8$^+$ thymocytes, indicating a potential impairment at the DN-to-DP transition in AgRP-Sirt1 KO mice. Next, we found that AgRP-Sirt1 KO mice displayed a significantly lower percentage of thymic CD4$^+$FoxP3$^+$ naturally occurring regulatory T (Treg) cells compared with control values (Fig. 1*D*). This difference was associated with impairment in the in vivo proliferation of thymus-derived Treg cells shown by significantly reduced ex vivo expression of the proliferating cell nuclear antigen (PCNA) in AgRP-Sirt1 KO mice. Because we have previously shown that the

Author contributions: G.M., N.D., and T.L.H. designed research; G.M., C.P., C.M., J.G.K., J.D.K., V.D.R., and M.O.D. performed research; M.O.D. and T.L.H. contributed new reagents/analytic tools; G.M., C.P., C.M., J.G.K., S.D., N.D., V.D.R., and T.L.H. analyzed data; and G.M. and T.L.H. wrote the paper.

The authors declare no conflict of interest.

*This Direct Submission article had a prearranged editor.

[1]To whom correspondence may be addressed. E-mail: gmatarese@unisa.it or tamas.horvath@yale.edu.

This article contains supporting information online at www.pnas.org/lookup/suppl/doi:10.1073/pnas.1210644110/-/DCSupplemental.

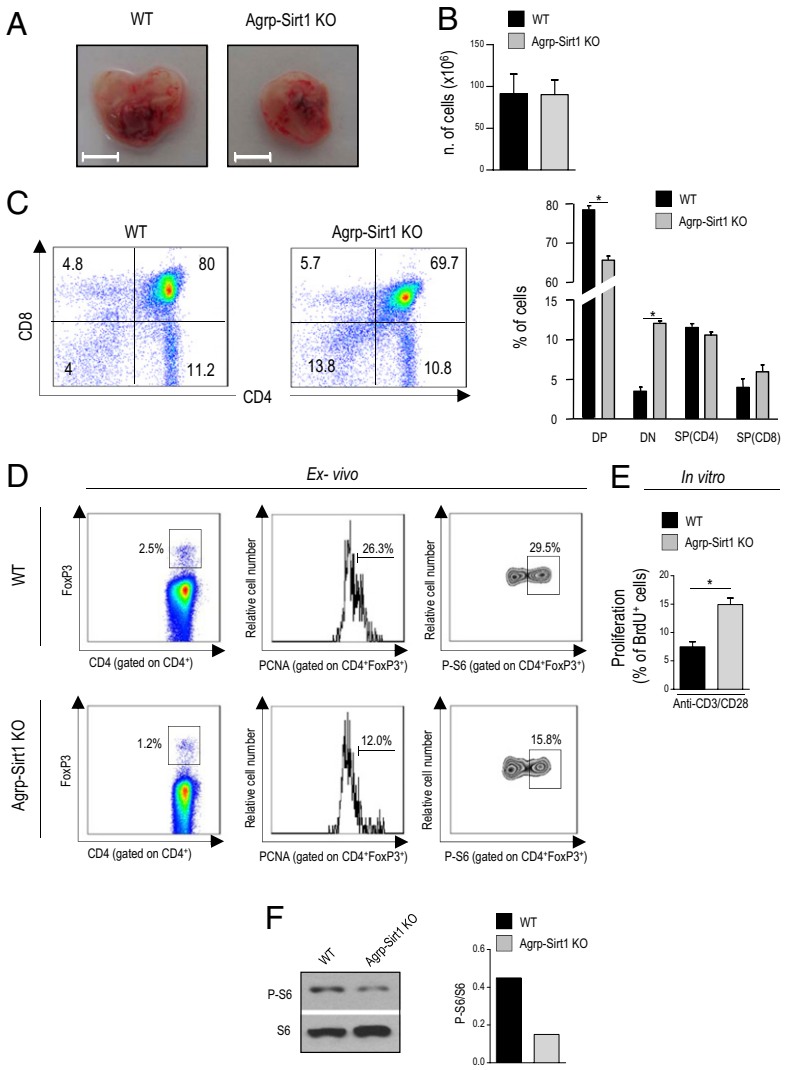

Fig. 1. Thymic phenotype and effects of selective ablation of Sirt1 in Agrp neurons in the generation of thymic-derived naturally occurring Treg cells. (*A*) Morphology of thymus from WT and AgRP-Sirt1 KO mice. (*B*) Cell numbers of thymocytes in WT (black columns) and AgRP-Sirt1 KO (gray columns) mice. Data are shown as mean ± SD ($n = 5$ mice/group). (*C*) CD4 and CD8 expression in the thymus from WT and AgRP-Sirt1 KO mice. One representative out of three independent experiments. (*D*) Ex vivo analysis of the percentage of Treg, PCNA, and S6 expression in Treg cells from the thymus of WT and AgRP-Sirt1 KO mice. ($n = 3$ mice/group, one representative out of three independent experiments). (*E*) Percentage of BrdU-positive cells upon anti-CD3/CD28 stimulation in thymic-derived Treg cells from WT (black column) and AgRP-Sirt1 KO (gray column) mice. The data are shown as mean ± SD ($n = 5$ mice/group; $^*P < 0.001$). (*F*) Immunoblot for P-S6 and its relative densitometric quantification in purified thymic-derived Treg cells from WT (black column) and AgRP-Sirt1 KO (gray column) mice. One representative out of three independent experiments.

mammalian target of rapamycin (mTOR) kinase plays a key role in the metabolic control of Treg cell responsiveness (17–20), we also analyzed S6 phosphorylation levels, a measure of mTOR pathway activity in the thymic Treg cell subset. In accordance with previous findings, impaired in vivo proliferation of thymic Treg cells in the AgRP-Sirt1 KO mice was associated with lower activity of mTOR pathway compared with controls (Fig. 1 *D* and *F*). Conversely, upon in vitro stimulation, Treg cells from AgRP-Sirt1 KO mice were not "classically anergic" like their control littermates, because they showed a lower proliferative profile in vivo and a reduced anergy in vitro upon CD3/CD28 stimulation (Fig. 1*E*).

AgRP-Sirt1 KO Mice Display Increased Activation of CD4$^+$ T Cells upon in Vivo Antigen Challenge. We next analyzed peripheral adaptive immune responses of CD4$^+$ T cells in immunized mice primed with complete Freund's adjuvant (CFA). Surprisingly, lymph node-derived T cells from AgRP-Sirt1 KO mice proliferated more robustly upon T-cell receptor (TCR)-mediated stimulation (with anti-CD3ε and 2C11 mAb) than those from their littermate controls (Fig. 2*A*). The increased proliferative profile of these cells in AgRP-Sirt1 KO mice was associated with significantly higher proinflammatory cytokine production compared with control values, including IL-2, IL-6, IL-17, IFN-γ, and TNF-α, whereas secretion of IL-4 and IL-5, both anti-inflammatory cytokines, was significantly lower, and there was also a tendency to decrease the amount of IL-10 (Fig. 2*B*) in the KO mice. These cytokine profiles correlated with the expression of cell-surface activation markers on CD4$^+$ T cells from control and AgRP-Sirt1 KO mice. The expression of activation markers such as CD25, CD54, and CD49d was significantly higher, together with their increased induction, upon TCR-mediated activation in AgRP-Sirt1 KO mice compared with controls (Fig. 2*C*). Finally, the molecular signaling analysis of the early activation events revealed an enhanced phosphorylation of ERK1/2 and S6, as well as a concomitantly more pronounced degradation of the cyclin-dependent kinase inhibitor p27^{Kip1} in T cells from AgRP-Sirt1 KO mice compared with controls (Fig. 2*D*).

AgRP-Sirt1 KO Mice Display a Discordant Suppressive Function of Naturally Occurring Treg Cells. To address whether these functional alterations in terms of increased proinflammatory activity in CD4$^+$ T cells was functionally related to an impairment in naturally occurring FoxP3$^+$ Treg cell number and function, we next analyzed peripheral lymph node-derived Treg cell compartments in antigen-challenged (immunized with CFA) mice. Ex vivo analysis of Treg cells in these animals revealed that AgRP-Sirt1 KO mice displayed an impairment in their homeostatic proliferation, as shown by reduced expression of PCNA in the lymph nodes (Fig. 3*A*). This phenomenon was accompanied by a reduced activity of the mTOR pathway (assessed as S6 phosphorylation), indicating an altered metabolic control of Treg cell proliferation in AgRP-Sirt1 KO mice (Fig. 3*A*). Interestingly, these phenomena

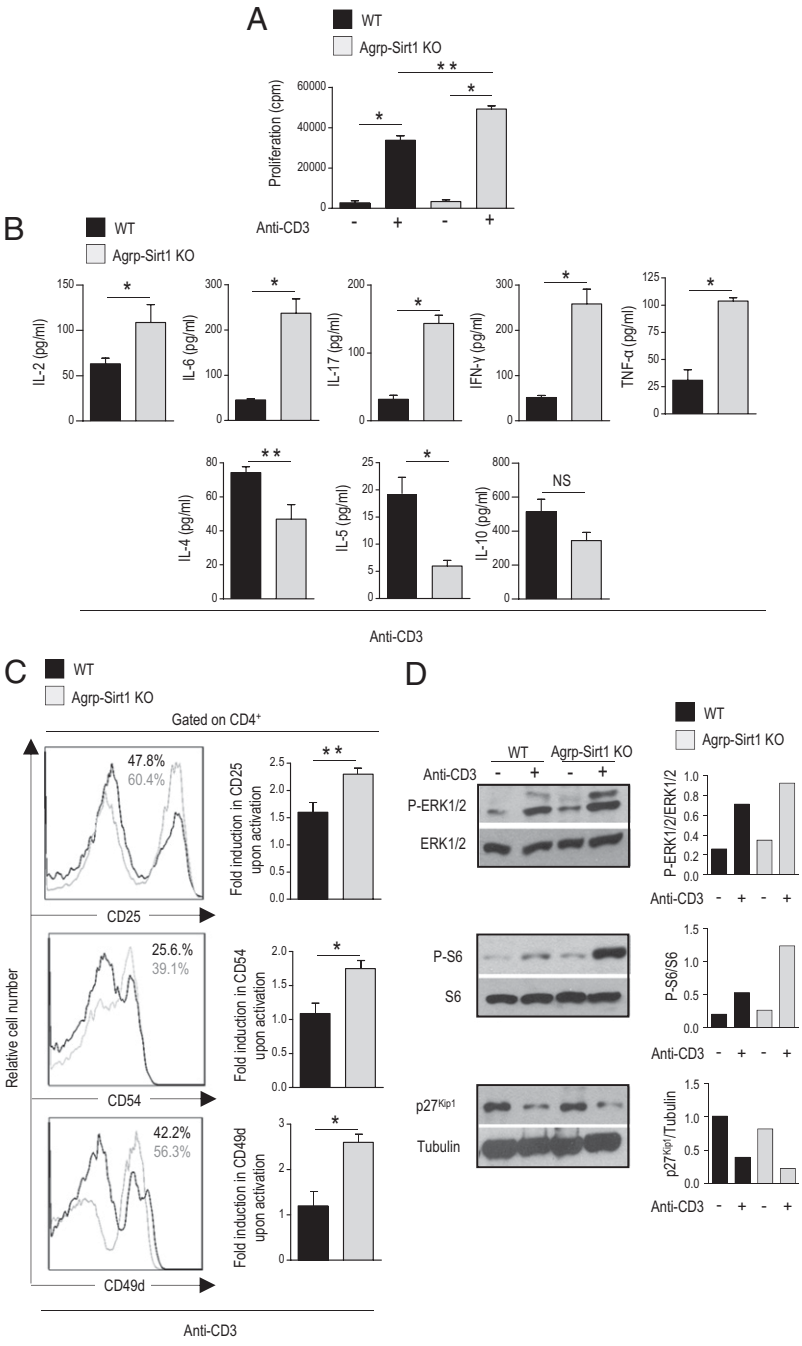

Fig. 2. Effect of selective Sirt1 ablation in AgRP neurons on the control of CD4$^+$ T-cell functions. (*A*) Proliferative response of lymph node-derived T cells from WT (black columns) and AgRP-Sirt1 KO (gray columns) mice, stimulated or not with anti-CD3 for 48 h. Data are shown as mean ± SD (n = 5 mice/group; *P < 0.0001, **P < 0.05). (*B*) IL-2, IL-6, IL-17, IFN-γ, TNF-a, IL-4, IL-5, and IL-10 production in cell supernatant from lymph node-derived T cells from WT (black columns) and AgRP-Sirt1 KO (gray columns) mice. The data are shown as mean ± SD (n = 5 mice/group; *P < 0.001, **P < 0.05; NS, not significant). (*C*) Activation markers (CD25, CD54, and CD49d) expression gated on CD4$^+$ T cells from WT (black histogram) and AgRP-Sirt1 KO (gray histogram) mice, stimulated with anti-CD3 after 36 h of culture. For each molecule the fold induction upon anti-CD3 stimulation is shown. Representative of five independent experiments. (*D*) Immunoblot for P-ERK1/2, ERK1/2, P-S6, S6, p27^{Kip1}, and tubulin on lymph node-derived T cells from WT and AgRP- Sirt1 KO mice, stimulated or not with anti-CD3 for 1 h. The graphs show the relative densitometric protein quantification of P-ERK 1/2, P-S6, and p27^{Kip1} specifically of the gels shown in Fig. 1*D* from WT (black columns) and AgRP-Sirt1 KO (gray columns) mice. One representative out of three independent experiments.

were revealed upon CFA immunization and were not observed in naïve AgRP-Sirt1 KO mice (Fig. S5). At a functional level we observed a "discordant" suppressive capacity in Treg cells from AgRP-Sirt1 KO mice; they were able to suppress proliferation of CD4$^+$CD25$^-$FoxP3$^-$ T-effector (Teff) cells evaluated as thymidine incorporation (Fig. S9 and Fig. 3*B*) but associated with a reduced capacity to suppress proinflammatory cytokine production by Teff. As shown in Fig. 3*B*, IL-2, IL-17, and IFN-γ produced by Teff cells were not inhibited by Treg cells from AgRP-Sirt1 KO mice compared with littermate controls (Fig. 3*B* and Fig. S9). To address the molecular mechanism linking the altered neuronal activity with the peripheral immune phenotype observed in AgRP-Sirt1 KO mice, we evaluated, as a measure of sympathetic tone, uncoupling protein 1 (UCP1) mRNA expression in both groups of mice. We observed that UCP1 level was significantly elevated in the brown adipose tissue (BAT) of AgRP-Sirt1 KO animals compared with controls (Fig. S10), and in vivo treatment with sympathetic blockers propranolol and SR59230A reduced UCP1 expression to a level comparable to that of control mice (Fig. S10). Interestingly, the analysis of the effect of sympathetic blockade on the immune phenotype of both WT and AgRP-Sirt1 KO mice revealed that propranolol and SR59230A in vivo treatment was able to reverse the impaired suppressive function of Treg cells (Fig. 3*B*). In agreement with the impaired suppressive capacity, purified Treg cells from AgRP-Sirt1 KO mice produced a significantly lower amount of regulatory anti-inflammatory cytokines such as IL-10 and TGF-β (Fig. 3*C*), both central cytokines involved in Treg suppressive functions (21, 22). This suggests that the observed impairment might be in part responsible for the altered suppressive activity detected in AgRP-Sirt1 KO mice, in terms of inhibition of proinflammatory secretion. Notably, no difference in IL-4 production was detected (Fig. 3*C*). Again, in vivo sympathetic

PHYSIOLOGY

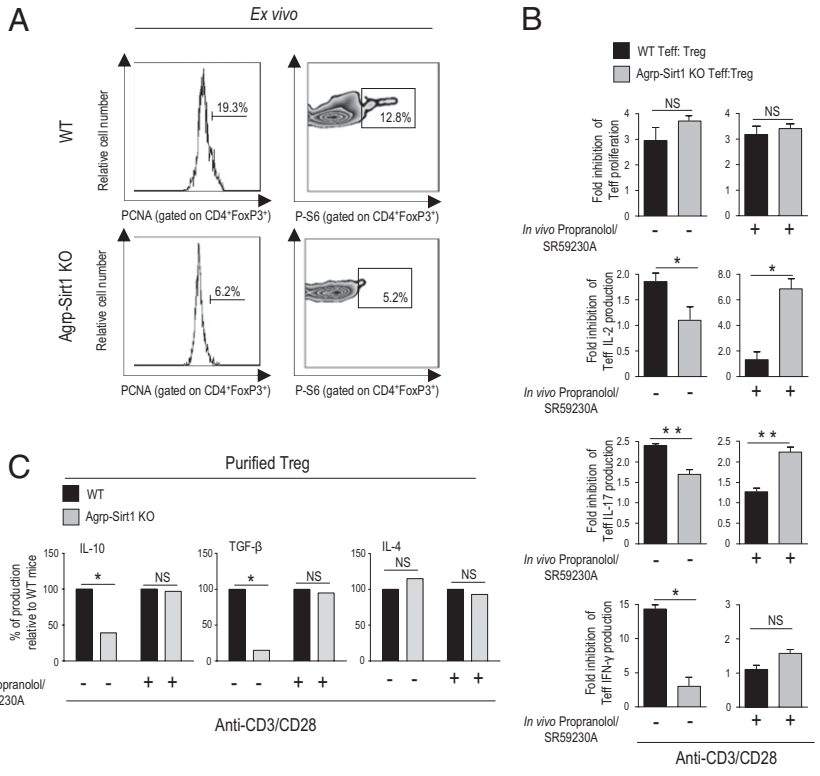

Fig. 3. Effect of selective Sirt1 ablation in AgRP neurons in the control of Treg cell functions. (*A*) Flow cytometry ex vivo analysis of PCNA (*Left*) and PS6 (*Right*) in Treg cells from the lymph nodes of WT and AgRP-Sirt1 KO mice. ($n = 3$ mice/group, representative of three independent experiments). (*B*) Proliferation, IL-2, IL-17, and IFN-γ production by Teff cells in coculture with Treg cells from WT and AgRP-Sirt1 KO mice treated or not in vivo with propranolol and SR59230A, upon anti-CD3/CD28 stimulation. The data are shown as mean ± SD ($n = 5$ mice/group; $^*P < 0.0001$, $^{**}P < 0.05$). (*C*) IL-10, TGF-β, and IL-4 production in purified Treg cells from WT (black columns) and AgRP-Sirt1 KO (gray columns) mice treated or not in vivo with propranolol and SR59230A, upon anti-CD3/CD28 stimulation. ($n = 5$ mice/group; $^*P < 0.001$; NS, not significant).

blockade was able to restore the production of anti-inflammatory IL-10 and TGF-β from AgRP-Sirt1 KO mice (Fig. 3*C*).

AgRP-Sirt1 KO Mice Display Enhanced Delayed-Type Hypersensitivity Responses and Increased EAE Susceptibility to Myelin Autoantigens. To determine the nature of the in vivo adaptive T-cell response in mutant Agrp-Sirt1 KO mice in the context of $CD4^+$-mediated T-cell responses and autoimmune disease susceptibility, we induced EAE and measured delayed-type hypersensitivity (DTH) responses against the myelin oligodendrocytic peptide $MOG_{35–55}$. Seven days after priming with the $MOG_{35–55}$ peptide emulsified in CFA, mice were challenged with 50 μg of $MOG_{35–55}$ injected intradermally in the footpad. The degree of local footpad swelling was measured as an indication of the DTH reaction. Typical DTH kinetics were observed and footpad swelling peaked between 48 and 72 h and subsided after 96 h (Fig. 4*A*). DTH responses to the $MOG_{35–55}$-priming epitope were significantly enhanced in AgRP-Sirt1 KO mice compared with littermate controls (Fig. 4*A*). In addition, mice were monitored up to 30 d for clinical signs of EAE. In agreement with the observed enhanced DTH reactivity, AgRP-Sirt1 KO mice showed an increased EAE susceptibility compared with normal control mice (Fig. 4*B*), as shown by increased inflammatory infiltrates of the CNS (Fig. 4 *C* and *D*). These data were associated with increased $MOG_{35–55}$-specific proliferation and inflammatory cytokine production by AgRP-Sirt1 KO mice (Fig. 4 *E* and *F*).

Discussion

Nutritional status, and metabolism in general, can affect peripheral immune responses. For example, fuel availability, through regulation of adipocytokines, controls inflammatory immune responses (23, 24). In this context, leptin, the adipocyte-derived hormone, seems to play an important role. Elevated leptin levels promote a proinflammatory state, an effect that likely relies on both central and peripheral modes of action (25–28). In contrast, fasting or chronic calorie restriction promotes anti-inflammatory processes, which occur while circulating leptin levels are low (25–28).

In the present study, we found that impairment of AgRP neuronal responses to metabolic cues by cell-specific knockdown of Sirt1 (4) resulted in a proinflammatory state, in which effector T-cell function is enhanced while regulatory T-cell activity is diminished, as suggested not only by an enhanced proinflammatory cytokine production in vitro, but also by an increased in vivo reactivity to self-myelin antigens. This proinflammatory immune phenotype emerged in animals despite the fact that they are leaner and have lower circulating leptin levels compared with their control littermates (4). These results suggest that the hypothalamic melanocortin system can exert control over peripheral immune responses independent of circulating leptin levels or adiposity.

AgRP neurons are crucial for hunger and adaptation to low energy availability (1, 2). Their primary actions on feeding, energy expenditure, and glucose metabolism are thought to be mediated by their GABAergic efferents to various hypothalamic and extrahypothalamic sites as well as via AgRP's effect on the melanocortin 4 receptors (29, 30). For feeding behavior, AgRP efferents in the parabrachial nucleus and paraventricular hypothalamic nucleus have been emphasized. However, there is an important role attributed to AgRP efferent-targeted arcuate nucleus proopiomelanocortin (POMC) neurons in many endocrine and autonomic effects of the melanocortin system (31–34). Indeed, we found that selective Sirt1 knockout in AgRP neurons, through impairing AgRP neuronal excitability, can disinhibit POMC neurons, leading to decreased feeding and increased energy expenditure of these animals (4). An increase in POMC neuronal activity can lead to elevated sympathetic tone through direct POMC efferents in the thoracic segments of the spinal cord. Because the immune system is under sympathetic control (35), we suggest that the altered immune phenotype observed in our AgRP-Sirt1 KO mice originated, at least in part, from the activity of the disinhibited POMC neurons. In line with this, we observed that UCP1 mRNA is significantly elevated in the BAT of AgRP-Sirt1 KO animals compared with littermate controls, suggesting an elevated sympathetic tone of these animals (Fig. S10). We then showed that in vivo sympathetic blockade abolished the difference in UCP1 mRNA levels as well as in suppressive capacity and cytokine production by Treg cells in AgRP-Sirt1 KO and control mice. This information, together with a recent paper by Luquet and coworkers (36), confirms our

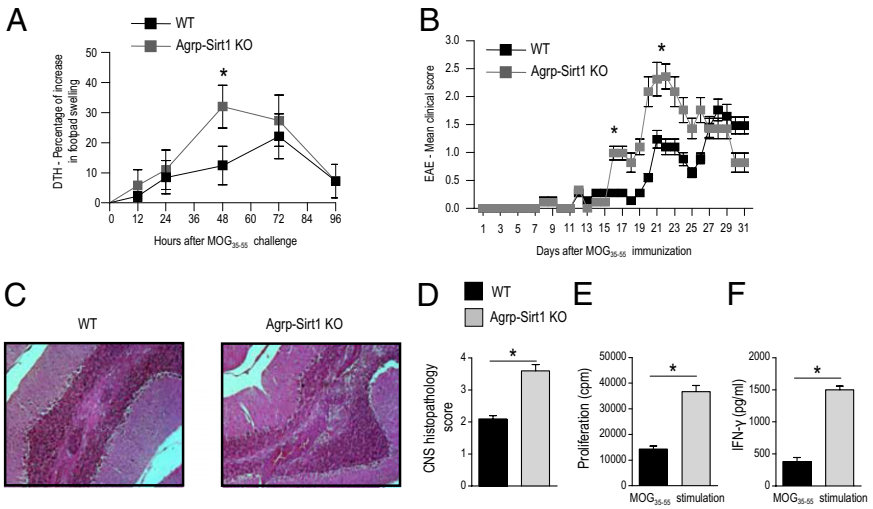

Fig. 4. Effect of selective Sirt1 ablation in AgRP neurons on DTH responses and EAE susceptibility. (*A*) Seven days after sensitization with $MOG_{35–55}$ in CFA, mice were challenged by injection of $MOG_{35–55}$ into the footpad and then assessed for DTH responses (footpad-swelling assay) 0, 12, 24, 48, 72, and 96 h later. Data are showing the means of percentage of increase ± SD of footpad-swelling responses ($n = 6$ mice/group; $^*P < 0.05$). (*B*) EAE mean clinical course and severity in AgRP-Sirt1 KO mice and WT control littermates. Mutant animals had a more severe clinical course than WT animals. One representative experiment ($n = 5$ mice/group; $^*P < 0.05$). (*C*) Inflammatory lesions in brain parenchyma from WT (*Left*) and AgRP-Sirt1 KO mice (*Right*) stained with hematoxylin and eosin. (Magnification, ×200.) (*D*) Summary of the inflammatory lesions in brain of WT and AgRP-Sirt1 KO mice. Results are expressed as the mean histological score ± SD ($n = 4–10$ sections/mouse) ($n = 5$ mice/group; $^*P < 0.05$). (*E*) $MOG_{35–55}$ peptide-specific proliferation and IFN-γ production (*F*) of lymph node cells from WT and AgRP-Sirt1 KO mice 20 d (peak of disease) after immunization. Data are shown as mean ± SD ($n = 5$ mice/group; $^*P < 0.001$).

suggestion that the sympathetic nervous system plays a crucial role in mediating the effect of impaired AgRP neuronal activity on the immune system. Elevated POMC tone in lean AgRP-Sirt1 KO animals reflects their "central perception" of relative satiety compared with control littermates. This is normally characteristic of overfed mice with elevated leptin levels, a state that also supports inflammation, enhanced activation of $CD4^+$ T cells, and a qualitative and quantitative reduction in Treg cells (19, 37, 38). Our results are also in line with the overall effect of sirtuins on the immune system (16) and suggest that AgRP neurons represent an important site of action of sirtuins to exert a systemic effect during low energy availability on the immune system. Finally, because the intracellular second messenger cAMP has a key role in mediating suppressive activity of Treg cells (39), in our system it would be interesting to monitor on hypothalamic neurons some cAMP-activating neurotransmitters such as the pituitary adenylate cyclase-activating polypeptide (39). Altered levels of such molecules could, at least in part, explain some of the results we observed in our AgRP-Sirt1 KO mice, particularly in the context of the observed reduced suppressive capacity of Treg cells.

In summary, our observations provide a unique role for hypothalamic AgRP neurons in integrative physiology. Our data support the notion that the CNS can affect immune functions (40, 41), which can supersede the predicted effects of circulating metabolic hormones, such as leptin. These results, together with our recent demonstration of specific behavioral and metabolic phenotypes of AgRP-Sirt1 KO animals (3, 4), suggest that traits of altered motivated behaviors and basic metabolic parameters can be predictors of adaptive immune system phenotypes.

Materials and Methods

Mice. We used the knockdown model of Sirt1 in the NPY/AgRP neurons previously described (4). Briefly, we used Cre/Lox technology to knock down the catalytic domain of Sirt1 in this population of cells. Transgenic mice expressing *Cre* recombinase selectively in the AgRP-expressing cells (42–44) were bred with mice harboring a targeted mutant Sirt1 allele (Sirt1*loxP*) (43). The Sirt1*loxP*/*loxP* mice contain *loxP* sequences flanking exon 4 of the Sirt1 gene, which encodes 51 amino acids of the Sirt1 catalytic domain. When bred with the *AgrpCre*+ mice, the deleted Sirt1 allele (Sirt1Δex4) transcribes a mutant protein that has no apparent residual Sirt1 activity or dominant negative effects (45, 46). We describe our data by referring to control (littermate Cre controls) and AgRP-Sirt1 KO mice. All animals were kept in temperature- and humidity-controlled rooms, in a 12/12-h light/dark cycle, with lights on from 7:00 AM to 7:00 PM. Food and water were provided for ad libitum consumption. All of the experiments were performed in animals 8–10 wk old. Experiments were conducted in accordance with the animal welfare guidelines under an approved protocol of the Istituto Superiore di Sanità, Roma, Italy.

Induction of EAE and DTH Responses (Footpad-Swelling Assay). For actively induced EAE, mice were immunized s.c. in the flank with 100 μL of CFA (Difco Laboratories) emulsified with 200 μg of $MOG_{35–55}$ peptide on day 0, and with 200 ng of pertussis toxin (Sigma) i.p. on days 0 and 1. Individual mice were observed daily for clinical signs of disease for up to 30 d after immunization. Mice were weighed and scored daily according to the clinical severity of symptoms on a scale of 0–6 by an experimenter "blinded" to their identity, with 0.5 points for intermediate clinical findings, as follows: grade 0, no abnormality; grade 0.5, partial loss of tail tonicity, assessed by inability to curl the distal end of the tail; grade 1, reduced tail tone or slightly clumsy gait; grade 2, tail atony, moderately clumsy gait, impaired righting ability, or any combination of these signs; grade 3, hind-limb weakness or partial paralysis; grade 4, complete hind-limb paralysis or forelimb weakness; grade 5, tetraplegia or moribund state; grade 6, death. The data were plotted as daily mean clinical scores for all animals in a particular treatment group. Scores of asymptomatic mice (score = 0) were included in the calculation of the daily mean clinical score for each group. The brains and spinal cords were dissected 20 d (peak of disease) after immunization and fixed in 10% formalin. Paraffin-embedded sections, 5 μm thick, from brains and spinal cords were stained with hematoxylin–eosin and investigated for evidence of inflammation. Sections from 4 to 10 segments per mouse were examined by one investigator blinded to the group's identity using a published scoring system for inflammation (47).

DTH responses to $MOG_{35–55}$ peptide during induction of disease were also quantitated using a time-dependent (12–96 h) footpad-swelling assay. Briefly, mice previously sensitized with $MOG_{35–55}$ in CFA on day 0 were challenged by s.c. injection of 50 μg of $MOG_{35–55}$ (in 50 μL of PBS) into the right hind footpad 10 d later. PBS alone was injected into the left footpad to serve as control for measurements. Footpad thickness was measured 0, 12, 24, 48, 72, and 96 h after challenge by an experimenter blinded to sample identity, using a caliper-type engineer's micrometer. Information on flow cytometric analysis, proliferation assays, cytokines measurement, Western blots and biochemical analyses, in vivo treatment with propranolol and SR59230A, and real-time PCR analysis can be bound in *SI Materials and Methods*.

Statistical Analyses. The Mann–Whitney *U* test was used for unrelated two-group analyses and the Kruskal–Wallis ANOVA test for three or more groups,

using StatView software (Abacus Concepts Inc.). Results are expressed as mean ± SD. P values < 0.05 were considered statistically significant.

ACKNOWLEDGMENTS. G.M. is supported by grants from the European Union Ideas Programme, European Research Council Starting Independent Grant "menTORingTregs" 310496, Telethon-Juvenile Diabetes Research Foundation Grant GJT08004, Fondi per la Ricerca di Base Medical Research in Italy Grant RBNE08HWLZ, and Ministero della Salute Grant GR-2010-2315414. T.L.H. is supported by the National Institutes of Health Director's Pioneer Awards DP1DK006850 and DK080000.

1. Luquet S, Perez FA, Hnasko TS, Palmiter RD (2005) NPY/AgRP neurons are essential for feeding in adult mice but can be ablated in neonates. *Science* 310(5748):683–685.
2. Gropp E, et al. (2005) Agouti-related peptide-expressing neurons are mandatory for feeding. *Nat Neurosci* 8(10):1289–1291.
3. Dietrich MO, et al. (2012) AgRP neurons regulate the development of dopamine neuronal plasticity and non food-associated behaviors. *Nat Neurosci* 5:1108–1110.
4. Dietrich MO, et al. (2010) Agrp neurons mediate Sirt1's action on the melanocortin system and energy balance: Roles for Sirt1 in neuronal firing and synaptic plasticity. *J Neurosci* 30(35):11815–11825.
5. Brachmann CB, et al. (1995) The SIR2 gene family, conserved from bacteria to humans, functions in silencing, cell cycle progression, and chromosome stability. *Genes Dev* 9(23):2888–2902.
6. Cohen HY, et al. (2004) Calorie restriction promotes mammalian cell survival by inducing the SIRT1 deacetylase. *Science* 305(5682):390–392.
7. Ramadori G, et al. (2008) Brain SIRT1: Anatomical distribution and regulation by energy availability. *J Neurosci* 28(40):9989–9996.
8. Liu Y, et al. (2008) A fasting inducible switch modulates gluconeogenesis via activator/coactivator exchange. *Nature* 456(7219):269–273.
9. Kaeberlein M, McVey M, Guarente L (1999) The SIR2/3/4 complex and SIR2 alone promote longevity in Saccharomyces cerevisiae by two different mechanisms. *Genes Dev* 13(19):2570–2580.
10. Lin SJ, Defossez PA, Guarente L (2000) Requirement of NAD and SIR2 for life-span extension by calorie restriction in Saccharomyces cerevisiae. *Science* 289(5487): 2126–2128.
11. Tissenbaum HA, Guarente L (2001) Increased dosage of a sir-2 gene extends lifespan in Caenorhabditis elegans. *Nature* 410(6825):227–230.
12. Rogina B, Helfand SL (2004) Sir2 mediates longevity in the fly through a pathway related to calorie restriction. *Proc Natl Acad Sci USA* 101(45):15998–16003.
13. Chen D, Steele AD, Lindquist S, Guarente L (2005) Increase in activity during calorie restriction requires Sirt1. *Science* 310(5754):1641.
14. Chen D, Guarente L (2007) SIR2: A potential target for calorie restriction mimetics. *Trends Mol Med* 13(2):64–71.
15. Steinman L (2004) Elaborate interactions between the immune and nervous systems. *Nat Immunol* 5(6):575–581.
16. Zhang J, et al. (2009) The type III histone deacetylase Sirt1 is essential for maintenance of T cell tolerance in mice. *J Clin Invest* 119(10):3048–3058.
17. Procaccini C, et al. (2010) An oscillatory switch in mTOR kinase activity sets regulatory T cell responsiveness. *Immunity* 33(6):929–941.
18. Procaccini C, Galgani M, De Rosa V, Matarese G (2012) Intracellular metabolic pathways control immune tolerance. *Trends Immunol* 33(1):1–7.
19. De Rosa V, et al. (2007) A key role of leptin in the control of regulatory T cell proliferation. *Immunity* 26(2):241–255.
20. Gerriets VA, Rathmell JC (2012) Metabolic pathways in T cell fate and function. *Trends Immunol* 33(4):168–173.
21. Chaudhry A, et al. (2011) Interleukin-10 signaling in regulatory T cells is required for suppression of Th17 cell-mediated inflammation. *Immunity* 34(4):566–578.
22. Rubtsov YP, et al. (2008) Regulatory T cell-derived interleukin-10 limits inflammation at environmental interfaces. *Immunity* 28(4):546–558.
23. Galic S, Oakhill JS, Steinberg GR (2010) Adipose tissue as an endocrine organ. *Mol Cell Endocrinol* 316(2):129–139.
24. Matarese G, La Cava A (2004) The intricate interface between immune system and metabolism. *Trends Immunol* 25(4):193–200.
25. Härle P, Straub RH (2006) Leptin is a link between adipose tissue and inflammation. *Ann N Y Acad Sci* 1069:454–462.
26. Matarese G, Procaccini C, De Rosa V, Horvath TL, La Cava A (2010) Regulatory T cells in obesity: The leptin connection. *Trends Mol Med* 16(6):247–256.
27. Procaccini C, Jirillo E, Matarese G (2012) Leptin as an immunomodulator. *Mol Aspects Med* 33(1):35–45.
28. La Cava A, Matarese G (2004) The weight of leptin in immunity. *Nat Rev Immunol* 4(5):371–379.
29. Renquist BJ, Lippert RN, Sebag JA, Ellacott KL, Cone RD (2011) Physiological roles of the melanocortin MC_3 receptor. *Eur J Pharmacol* 660(1):13–20.
30. Ghamari-Langroudi M, Srisai D, Cone RD (2011) Multinodal regulation of the arcuate/paraventricular nucleus circuit by leptin. *Proc Natl Acad Sci USA* 108(1):355–360.
31. Schwartz MW, Woods SC, Porte D, Jr., Seeley RJ, Baskin DG (2000) Central nervous system control of food intake. *Nature* 404(6778):661–671.
32. Cowley MA, et al. (2001) Leptin activates anorexigenic POMC neurons through a neural network in the arcuate nucleus. *Nature* 411(6836):480–484.
33. Cone RD (2006) Studies on the physiological functions of the melanocortin system. *Endocr Rev* 27(7):736–749.
34. Elmquist JK, Ahima RS, Elias CF, Flier JS, Saper CB (1998) Leptin activates distinct projections from the dorsomedial and ventromedial hypothalamic nuclei. *Proc Natl Acad Sci USA* 95(2):741–746.
35. Bhowmick S, et al. (2009) The sympathetic nervous system modulates CD4(+)FoxP3(+) regulatory T cells via a TGF-beta-dependent mechanism. *J Leukoc Biol* 86(6): 1275–1283.
36. Joly-Amado A, et al. (2012) Hypothalamic AgRP-neurons control peripheral substrate utilization and nutrient partitioning. *EMBO J* 31(22):4276–4288, 10.1038/emboj.2012.250.
37. Feuerer M, et al. (2009) Lean, but not obese, fat is enriched for a unique population of regulatory T cells that affect metabolic parameters. *Nat Med* 15(8):930–939.
38. Cipolletta D, et al. (2012) PPAR-γ is a major driver of the accumulation and phenotype of adipose tissue Treg cells. *Nature* 486(7404):549–553.
39. Bodor J, et al. (2012) Cyclic AMP underpins suppression by regulatory T cells. *Eur J Immunol* 42(6):1375–1384.
40. Tschöp J, et al. (2010) CNS leptin action modulates immune response and survival in sepsis. *J Neurosci* 30(17):6036–6047.
41. Tanaka M, et al. (2011) Role of central leptin signaling in the starvation-induced alteration of B-cell development. *J Neurosci* 31(23):8373–8380.
42. Kaelin CB, Xu AW, Lu XY, Barsh GS (2004) Transcriptional regulation of agouti-related protein (Agrp) in transgenic mice. *Endocrinology* 145(12):5798–5806.
43. Xu AW, et al. (2005) Effects of hypothalamic neurodegeneration on energy balance. *PLoS Biol* 3(12):e415.
44. Xu AW, et al. (2005) PI3K integrates the action of insulin and leptin on hypothalamic neurons. *J Clin Invest* 115(4):951–958.
45. Li H, et al. (2007) SirT1 modulates the estrogen-insulin-like growth factor-1 signaling for postnatal development of mammary gland in mice. *Breast Cancer Res* 9(1):R1.
46. Cheng HL, et al. (2003) Developmental defects and p53 hyperacetylation in Sir2 homolog (SIRT1)-deficient mice. *Proc Natl Acad Sci USA* 100(19):10794–10799.
47. Constantinescu CS, et al. (1998) Antibodies against IL-12 prevent superantigen-induced and spontaneous relapses of experimental autoimmune encephalomyelitis. *J Immunol* 161(9):5097–5104.